ELSEVIER

Polymer 43 (2002) 6159–6167

polymer

www.elsevier.com/locate/polymer

Mechanical properties of polyacrylic–titania hybrids—microhardness studies

F.X. Perrin*, Vannhan Nguyen, J.L. Vernet

Laboratoire de Chimie Appliquée, Université de Toulon et du Var, BP132, 83957 La Garde Cedex, France

Received 26 March 2002; received in revised form 30 July 2002; accepted 7 August 2002

Abstract

Organic/inorganic (O/I) hybrid materials containing 4.6–19.5 wt% of titania have been prepared using poly(methylmethacrylate-*co*-butyl methacrylate-*co*-methacrylic acid) and acetic acid modified tetrabutyl titanate as the sol–gel precursor. The microhardness (MH) of the acrylic–titania hybrids was investigated. The influence of TiO_2 content on MH is particularly discussed and compared with similar results obtained with other O/I composite materials. The hybrid material filled with 10.7 vol% of titania is more than twice harder than the polymer matrix. This strong hardening effect is ascribed to the homogeneous dispersion of the filler in the polymer matrix and to the strong filler–polymer interactions. Hardness was found to be related to the density of hybrids through a semi-logarithmic relationship. Besides, the glass transition temperature T_g of hybrids was determined from temperature dependence of hardness. The T_g evolution with titania content is discussed with reference to solvent extraction results. Finally, the time-dependence of MH reveals that the inorganic network more strongly affects the creep behavior of the polymer above T_g than below T_g. © 2002 Published by Elsevier Science Ltd.

Keywords: Hybrid composite; Sol–gel reactions; Microhardness

1. Introduction

Hybrid organic/inorganic (O/I) materials prepared by the sol–gel process have a great potential in many important applications, such as non-linear optics, biosensors or hard coatings [1–3]. The last decade saw an extensive work to produce materials with an optimized combination of the best properties of polymers with the best properties of ceramics [4,5]. Recently, the protection of metals against corrosion with hybrid materials has been reported with epoxy [6], linseed oil [7] and polymethylmethacrylate [8] matrix resins. In view of corrosion protection, adherence and especially wet-adherence have often been referred as the key property controlling the long-term efficiency of the protection [9]. In O/I hybrids, a strong adherence should result from the covalent interactions between the oxide layer present at the metal substrate surface and the partially hydrolyzed metal alkoxide. Such interactions have been previously reported with pure inorganic materials [10]. The polymer component in O/I hybrid should impart two major advantages in terms of protective coatings application. Actually, the shrinkage inherent to the sol–gel process usually induce generalized cracking of the pure brittle ceramic coating when thickness exceeds 1 μm. Then, the polymer component in hybrids is believed to impart sufficient flexibility to attain films with thickness >10 μm. The second advantage concerns the impregnation of open pores by the polymer that should reduce coating porosity, hence giving a better barrier to diffusion.

Apart from the quality (i.e. adherence) of the metal/coating interface, the bulk properties and especially the mechanical properties of the material must also be considered when dealing with the quality of a coating/metal system. For example, hardness can be directly related with wear resistance, a fundamental requirement in several coatings applications. During the last two decades, more and more investigations showed that microhardness (MH) was a relevant tool to better understand the morphology–property relationship of polymers [11–18]. So far, most fundamental MH studies concern semi-crystalline polymers and more specifically the crystal size and perfection [11], the kinetics of crystallization (poly(ethylene naphthalene-2,6-dicarboxylate) (PEN) [12], poly(ethyleneterephthalate) (PET) [13] or PET/PEN blends [14]), the detection of polymorphic changes (in isotactic polypropylene [15]),

* Corresponding author. Tel.: +33-494-142580; fax: +33-494-142448.
E-mail address: perrin@isitv.univ-tln.fr (F.X. Perrin).

0032-3861/02/$ - see front matter © 2002 Published by Elsevier Science Ltd.
PII: S0032-3861(02)00543-8

Table 1
Organic–inorganic composition and bulk density of the AP-TiO_2 hybrid materials

Sample code	(Ti)/(COOH)[a] molar ratio	TiO_2		Bulk density (g/cm^3)
		wt%[b]	vol%[c]	
AP	0	0	0	1.09
AP-2	2	4.6	2.3	1.12
AP-2.5	2.5	5.7	2.9	1.13
AP-4	4	8.8	4.6	1.16
AP-6	6	12.7	6.8	1.19
AP-8	8	16.3	8.8	1.21
AP-10	10	19.5	10.7	1.23
Pure sol–gel titania	–	100	100	2.24

[a] Carboxylic groups from the polymer.
[b] Calculated percentage assuming 100% conversion of metal alkoxide to TiO_2 and totally removed AcA.
[c] Calculated from the relationship: $\text{vol\%} = \text{wt\%} \times d_{\text{hybrid}}/d_{\text{titania}}$ where wt% is the weight percent titania content, d_{hybrid} is the density of the hybrid material and d_{titania} is the density of the pure sol–gel titania.

structure–property relationship in polymer blends (poly(ethylene)/poly(propylene) blends [16]). Studies concerning amorphous glassy polymers are more scarce. For amorphous polymers, MH revealed to be a convenient tool to detect the glass transition temperature T_g [17]. More recently, Fakirov et al. [18] proposed a unique linear relationship between the room temperature hardness and T_g of amorphous polymers distinguished by single main-chain bonds.

Recently, we reported the preparation of acrylic terpolymer/titania hybrids from poly(methylmethacrylate-*co*-butyl methacrylate-*co*-methacrylic acid) (poly(MMA-BMA-MA)) and acetic acid (AcA) modified titanium butoxide precursor [19]. The addition of AcA was found to avoid both the formation of a tridimensional gel before hydrolysis of the polymer–alkoxide mixture and the TiO_2 precipitation when water is added. Although AcA competes with the active groups of the polymer (MA units) as a complexing agent of the alkoxide, bidentate chelating bonds between MA and titanium still occur, hence ensuring strong interactions between the organic and inorganic components [19].

So far, none thorough investigation concerns MH study of O/I hybrids prepared by the sol–gel process. The aim of this work is to extend the use of MH on such materials investigating the effect of titania filler on the mechanical properties of a poly(MMA-BMA-MA) terpolymer (AP). The influence of temperature on MH and the time-dependent part of the plastic deformation of hybrids will particularly be discussed.

2. Experimental

2.1. Materials

The acrylic polymer (AP) employed in this investigation was a random terpolymer of methylmethacrylate (MMA), *n*-butyl methacrylate (BMA) and methacrylic acid (MA) supplied by ICI. The composition of AP was determined from NMR ^{1}H spectra and was found to be 16 mol% MMA–80 mol% BMA–4 mol% MA [19]. Molecular weight from GPC determination: $\text{Mn} = 127,100\ \text{g/mol}$, polydispersity = 1.39 (based on PMMA standards).

Toluene (from SdS with $H_2O < 0.05\%$), tetrabutyltitanate (Aldrich, 97%) and AcA (from Acros) were used without further purification.

The water used for the sol–gel process was purified by means of a Millipore Milli-Q system.

2.2. Preparation of hybrids

In a typical procedure, AcA was added to a solution of AP in toluene (15 wt%) to give a molar ratio AcA/Ti = 3 in the final hybrid. The AP–AcA solution was added dropwise to the tetrabutyltitanate solution (15 wt% in toluene) with vigorous stirring. After additional stirring for 1 h, a solution of water in butanol (10 wt%) was slowly added to the homogeneous sol with a molar ratio $H_2O/Ti = 4$. The mixture was stirred for 1 h and poured into a Teflon mould. Upon successive drying 4–5 days at room temperature and under vacuum at 80 °C for 1 day, semi-transparent 200–300 μm thick films were obtained. Before hardness measurements, each sample was further annealed at room temperature in a desiccator for 1 month (see Section 3.1). Table 1 shows the composition of the final hybrids and their density (determined by Archimedes' method on a microbalance [19]).

A poly(MMA-BMA-MA)/TiO_2 (10.7 vol% TiO_2) film was also prepared by ultrasonically mixing a viscous solution of AP in toluene (40 wt%) with 200 nm TiO_2 powder (Acros). The resulting mixture was poured into a Teflon mould and dried for 1 day at 80 °C to give the so-called conventional composite film.

2.3. Techniques

Glass transition temperatures of the terpolymer were

determined by differential scanning calorimetry (DSC) on a Setaram apparatus. Samples of about 30 mg were heated at a rate of 10 K/min from -60 °C up to $T_g + 50$ °C, then cooled down to -60 °C and finally cycled again following the same procedure. The T_g was taken from the second run as the temperature where half of the increment in specific heat had occurred (midpoint temperature). Each sample was run twice and the average of two T_g values were reported.

The Vickers hardness measurements were performed at room temperature (≈23 °C) otherwise stated with a FM7 Testwell microhardness tester. The hardness in MPa was determined as $Hv = 1854F/d^2$ where F is the applied load (in mN) and d is the length of the diagonal (in μm). The average value from at least five indentation tests was systematically calculated. The maximum scatter typically ranges between 1 and 3% of the hardness value. For the sake of clarity, error bars are omitted in the figures. The variation of hardness as a function of load was performed over the range 98–980 mN. Afterwards, all measurements were carried out with a load of 245 mN. The indentation time was fixed at 15 s otherwise stated (creep study) and was considered sufficiently low to minimize for the creep effect. The temperature dependence of MH was also investigated setting the samples on a heating plate whose temperature is kept constant by a control circuit.

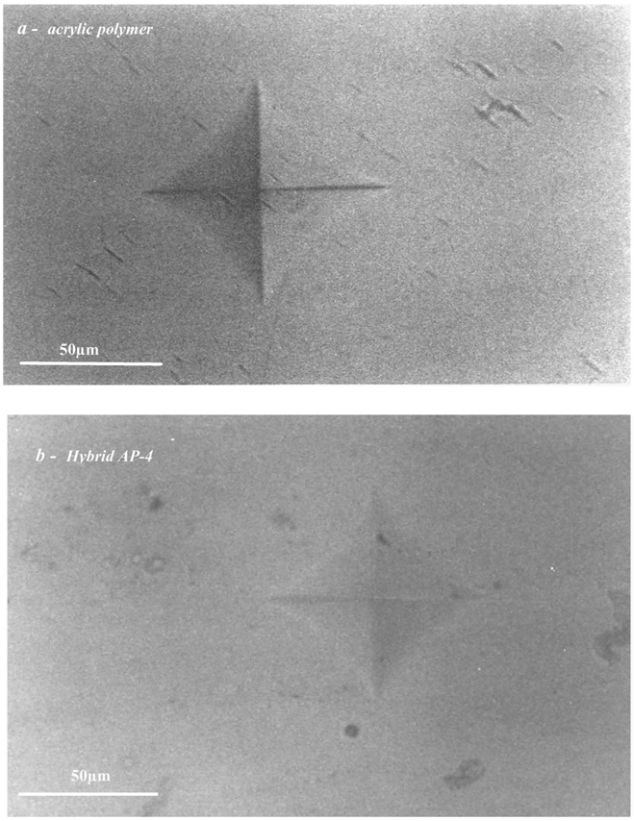

Fig. 1. Photograph of the Vickers microindentation obtained with a load of 0.245 N: (a) the AP; (b) the hybrid AP-4.

3. Results and discussion

The geometry of the Vickers indenter allows to relate the measured diagonal length d and the indentation depth thickness t with Eq. (1):

$$d = \frac{2\cos 16^\circ\, t}{\cos 74^\circ} \approx 7t \quad (1)$$

In this work, the calculated penetration depth ranged ca. between 5 and 15 μm. Measuring the intrinsic hardness of films is known to require films with thickness 10-fold higher than the penetration depth of the indenter [20]. Here, the latter condition is largely attained. Typical photographs of microindentations are presented in Fig. 1. Both on the polymer (Fig. 1(a)) and hybrid materials (Fig. 1(b)), Vickers indents show curved edges relative to elastic recovery along the sides as the indenter is retrieved. Such a difference with the ideal square indent is a common feature of polymeric materials [21]. The greater recovery along the direction at 45° of the two diagonals can be explained by the sharp edges of the Vickers indenter that induce strong stresses that limit the elastic recovery of the edges on the measured diagonal length d.

3.1. Hardness–load dependence

The effect of load on the MH is shown in Fig. 2 for the AP and the AP-4 hybrid film as a function of the curing time at 80 °C. For samples dried over 24 h, the measured hardness appears to be independent of the applied load, as could be anticipated by the geometrical similarity of the Vickers indentation mark. For drying times lower than 24 h, hardness of the samples are clearly load-dependent. The measured hardness decreases with an increase in the test load. It is noteworthy that most metals and ceramics exhibit such a load-dependent hardness which is usually referred as *indentation size effect* (ISE). Materials with a ductile behavior, such as metals normally display MH, which decreases as the load is increased. The origin of the ISE remains unclear even though several explanations have been

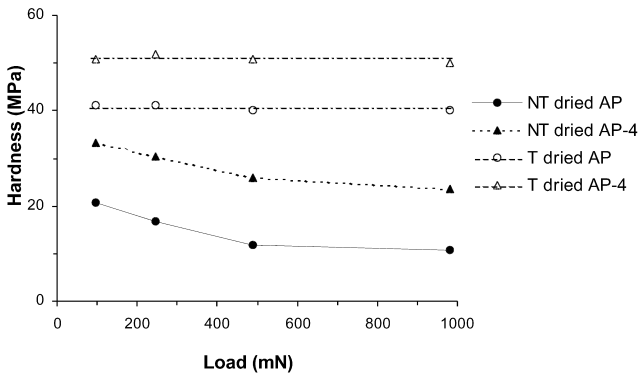

Fig. 2. Effect of the applied load on the measured hardness of the AP and hybrid AP-4. NT dried and T dried mean non-totally dried (1 h at 80 °C) and totally dried (24 h at 80 °C), respectively.

proposed. These proposals include either limitations in experimental conditions (low resolution of the objective lens [22], work hardening [23] or softening generated during the surface preparation [24]) or intrinsic structural factors of the material (work hardening during indentation [25], indentation elastic recovery [25], grain size effect [26]).

Here, the presence of residual solvents or other low molar mass molecules (water, alcohol, weakly bound acetate ligands, etc.) is believed to be more detrimental with respect to the Young's modulus of the material (decrease in E) than to its yield stress (also a decrease in σ_y). Therefore, the non-totally dried samples would have higher σ_y/E ratios and thus a higher part of elastic strain as compared to the totally dried samples. Since the plastic strain contribution decreases with a decrease in the indent volume, the observed decrease in hardness with an increase in the test load can be ascribed to a stronger elastic recovery of the diagonal d for the lower test loads. Such a load dependence is not observed for the totally dried samples owing to their lower σ_y/E ratio (lower contribution of elastic strain) that results in an insignificant recovery of the diagonal length.

3.2. Effect of the storage time at room temperature

All hybrid materials were dried 4 days at room temperature and next 1 day at 80 °C. The initial room temperature drying was found to impede cracking of the films due to a too fast evaporation of volatile species. The treatment at 80 °C (above the T_g of the polymer) was carried out in order to complete both the evaporation of volatile species (mostly alcohol and toluene) and the condensation reactions of the sol–gel process. After these both treatments, the films were stored in a desiccator at room temperature and the hardness of the films was followed as a function of the curing time. The results are shown in Fig. 3. As expected, a strong increase of hardness is observed during the curing at 80 °C. More interestingly, hardness of the materials goes on slowly increasing during their storage in the desiccator at room temperature. Hardness reaches a constant value after ca. 25 days at room temperature. Since this effect is also observed on the AP, it cannot be ascribed to the ending of the sol–gel process. A more reasonable assumption would be the slow ordering of the polymer chains in a more compact molecular packing (physical aging). In order to confirm the latter hypothesis, further room temperature annealed polymer and hybrid samples were heated few minutes above their glass transition temperature (80 °C): the room temperature hardness measured straight after such a treatment was found to be far below the measured hardness of the so-called *crude* room temperature annealed samples. From these results, it is obvious that a careful control of the thermal history of the samples is necessary so that all available information from hardness measurements be meaningful. That is why, all samples were stored 30 days at room temperature before hardness measurements.

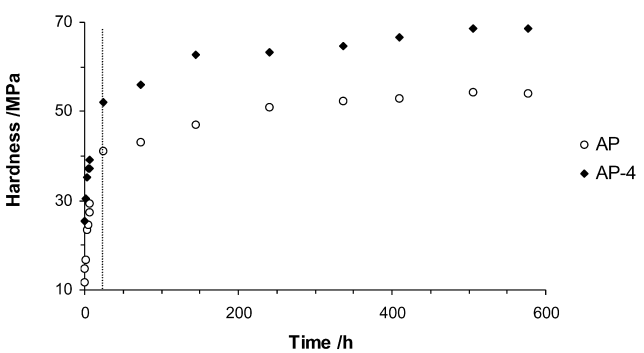

Fig. 3. Hardness values of the AP and hybrid AP-4 versus drying time. The dotted vertical line separates the 80° initial curing stage from the room temperature curing stage.

3.3. Hardness–T_g of the acrylic polymer

Based on data obtained with a number of commercial amorphous polymers, Fakirov et al. [18] found a unique linear relationship between the room temperature measured Vickers hardness (Hv) and T_g,

$$\text{Hv (MPa)} = 1.97T_g\text{ (K)} - 571. \quad (2)$$

This expression appears only valid for polymers mainly containing single bonds in the main chain. Substituting the measured T_g of 323 K (midpoint temperature determined from a second DSC run) in Eq. (2) gives a hardness value of 65 MPa. The measured hardness of 52 MPa appears acceptable, considering the discrepancy between individual experimental data used to determine coefficients in Eq. (2) and calculated ones [18]. This confirms the unique character of Eq. (2), adding a new AP to the previously given data [18].

3.4. Influence of filler content

Fig. 4 shows that the hardness of hybrids increases linearly with the amount of titania. Then, MH can be well

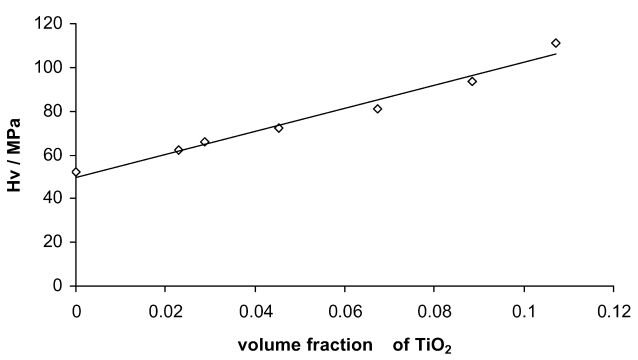

Fig. 4. Effect of filler volume fraction on the hardness of hybrids.

described by the simple additivity law (the so-called Rice's model developed for nanocomposites [27]):

$$Hv = Hv_1\phi + Hv_2(1 - \phi) \quad (3)$$

where Hv_1 and Hv_2 represent the individual hardness values of the titania network and the terpolymer, respectively, and ϕ is the volume fraction of the titania network. The straight line extrapolates for $\phi = 1$ at $Hv_1 \sim 574$ MPa. The latter value is far below the measured hardness of the pure sol–gel prepared titania material which is 1120 ± 40 MPa. Actually, the linear relationship (Eq. (3)) between Hv and ϕ has been determined with fairly low titania amounts (0–10.7 vol%) and it can be no longer valid for higher titania content. In the low titania concentration region, the observed increase in the resistance to flow results from titania–polymer interaction and thus show a linear dependence with the titania content. Here, in the transparent hybrids, titania is dispersed in the polymer matrix at a nanometric level. Therefore, the filler–filler interactions are believed to play no significant part to the resistance to flow of the materials. If the volume fraction of titania would exceed the three-dimensional percolation threshold (superior to 15 vol% for a disordered system), an infinite cluster of titania might be formed. Then, the harder titania component would be able to support the stress and the polymer matrix would play only a minor role. That would likely result in a discrepancy between the measured hardness and the hardness calculated from the Rice's model. Since in this work, the volume fraction of titania is far below the percolation threshold, such a discrepancy in the Rice's model is not observed.

The inclusion of $CaCO_3$ powder in a HDPE matrix was found to involve unsignificant increase in hardness when the filler content is inferior to 10 vol% [28]. Recently, the effect of MH of functionally graded polymer composites based on an epoxy resin matrix and hard SiC filler particles ($Hv = 31,380$ MPa) was also investigated [29]. MH is found to increase from 210 MPa for the unreinforced matrix to 270 MPa for a 10.7 vol% filled matrix, that is, an increase of $\approx$28%. Here, the hybrid material filled with 10.7 vol% of titania ($Hv \sim 111$ MPa) is more than twice harder than the polymer matrix ($Hv \sim 52$ MPa). The difference in the effect of filler on the hardness of composites is likely due both to the different particle size of the fillers and to the difference in the interfacial adhesion. $CaCO_3$ powder and SiC particles have an average particle size of 5.53 [28] and 9 μm [29], respectively, while all TiO_2 particles are below 0.4 μm. Therefore, the filler–polymer interface is much more important in the latter case, hence resulting in a better efficiency of the hardening effect of the fillers. On the other hand, the relatively weak interfacial adhesion of the $CaCO_3$/HDPE composites [28] gives little importance to reinforcement at low volume fractions of fillers. At volume fractions of $CaCO_3$ above 10–20%, filler–filler interactions causes the resistance to flow to increase significantly. Conversely, the strong hardening effect observed even with low titania content in the hybrids materials is another evidence (indeed, previous extraction results gave a percentage of cross-linked polymer up to ca. 70% [19]) that the mineral network is strongly connected to the AP.

The hardness of the pure sol–gel titania can be compared to the hardness of titania network available in the literature. Only Mohs hardness for the three crystalline forms of titania (brookite, anatase and rutile) are available and give Mohs hardness number M between 5.5 and 6.5 [30]. Since both the scratching hardness process (Mohs scale) and the static indentation process (with a Vickers indenter for instance) are determined primarily by the plastic properties of the material, some attempts were carried out to correlate the Mohs hardness M and the Vickers hardness Hv [31]. From fig. 25 in Ref. [31], the following relationship can be deduced: Hv (MPa) = 310.6 exp(0.461 M). Then, the Vickers hardness of crystalline titania is approximately 4940 MPa. This value is more than 4-fold higher than the hardness of our pure sol–gel titania network. This result can be explained by the amorphous nature (and so, less dense structure) of the sol–gel titania network. Moreover, organic ligands (mostly bidentate chelating acetate ligands [32]) still present in the dried sol–gel titania must have a softening effect and increase the discrepancy with the hardness of crystalline titania.

Besides, Fig. 5 shows that the additivity law of volumes applies to the hybrids materials in the whole titania concentration range 0–100% (a linear fitting with $r^2 > 0.998$ is found). In the low range 0–10.7 vol% of TiO_2, hardness is found to be related to the density of the hybrid materials (curve not shown) through the relation: $\ln Hv \times (MPa) = 5.04\rho\,(g/cm^3) - 1.54 (r^2 > 0.98)$. The hardness values have already been linked to the material density using such a logarithmic relation for different material compaction [33].

Contrary to the polymer film and the conventional poly(MMA-BMA-MA)/TiO_2 composite film, the hybrid film does not flow under its weight when it is hold upright at 150 °C. This reveals the strong interactions between the inorganic network and the AP in the hybrid material. More quantitative results concerning the effect of the titania

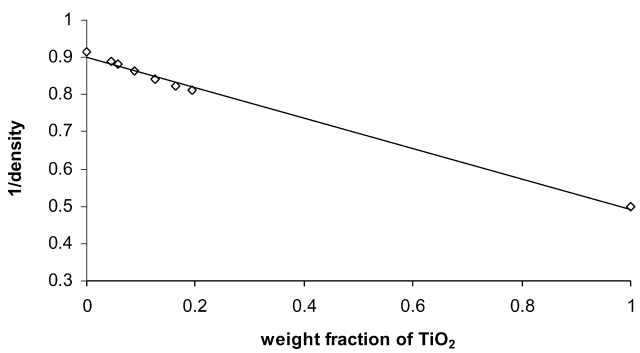

Fig. 5. The inverse of density of hybrids as a function of weight fraction of titania.

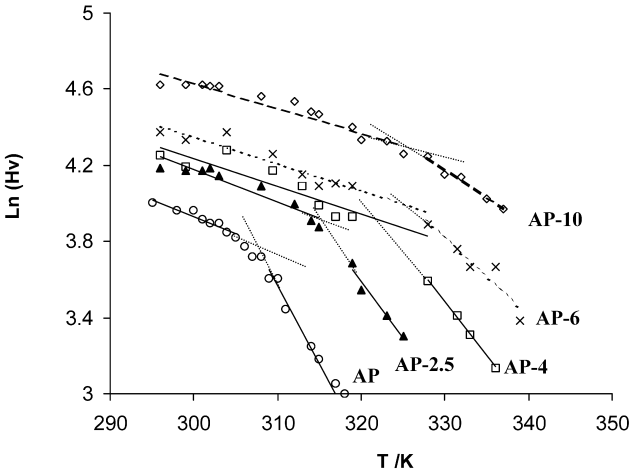

Fig. 6. log Hv as a function of temperature for the hybrid materials and the amorphous terpolymer.

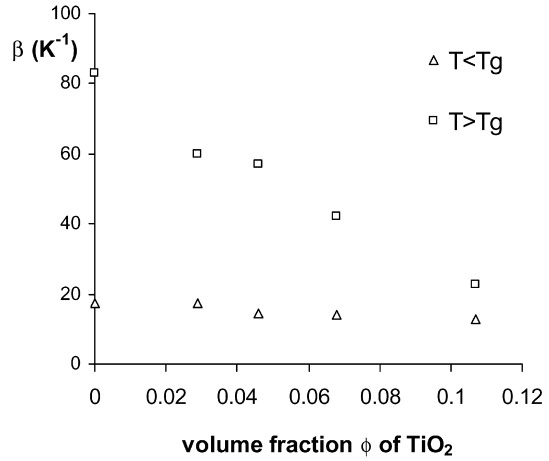

Fig. 7. Coefficients of thermal softening as a function of the titania content in hybrid materials.

network can be achieved through hardness–temperature dependence and creep measurements.

3.5. Temperature dependence

For all the investigated hybrids, MH decrease is found to follow the same exponential law as one found for semi-crystalline [17,34] or amorphous polymers [12,17] (Fig. 6):

$$Hv = Hv_0 \exp[-\beta T] \quad (4)$$

where Hv_0 is the hardness of the material at 0 K and β the so-called coefficient of thermal softening. The indentation hardness has been found to be a valuable tool to estimate the glass transition in amorphous polymers [17]. Below the T_g, Eq. (4) is valid with a coefficient of thermal softening β characteristic of the glass state while above the T_g, Eq. (4) is also valid but with a higher β value characteristic of the rubber state. Table 2 shows the β coefficients for the investigated hybrid materials and for the unfilled polymer. The values determined with the terpolymer AP are of the same order of magnitude than data obtained for other amorphous polymers [17]. The β coefficients both before and after the T_g are found to decrease with an increase in filler content of the hybrid materials. However, the effect is much more pronounced in the rubber state of the polymer (Fig. 7). Above the T_g, the rate of MH decrease with temperature is ca. four times lower with a 10.7 vol% filled hybrid than the rate measured on the pure polymer and it is not far from the rate measured on the pure polymer in the glassy state.

Table 2
Glass transition temperature T_g determined from different techniques and coefficient of thermal softening for the hybrid materials

Sample	$\beta \times 10^3$ (K^{-1})		T_g (K)	
	$T < T_g$	$T > T_g$	MH[a]	DSC[b]
AP	17.5	82.9	307 (305[c])	316 (305–309)
AP-2.5	17.2	60.0	314	–
AP-4	14.6	57.0	322	–
AP-6	14.0	42.3	325	–
AP-10	12.9	22.6	327	–

[a] T_g determined from hardness measurements at different temperatures under a constant loading time (0.25 min) except footnote b.
[b] Midpoint temperature determined from the second DSC run (see details in Section 2). T_g calculated from the Fox equation (first value) and T_g calculated from a simple weighted average of the T_g's of the component homopolymers (second value) is also indicated in brackets. The T_g values for poly(MMA), poly(BMA) and poly(MA) homopolymers used in the calculations were 378, 293 and 501 K, respectively (taken from Polymer Handbook [35]). T_g of the hybrids not determined due to strong broadening and decrease in intensity of the T_g profile.
[c] T_g determined from creep measurement at different temperatures (see text for details).

Although the discontinuity of thermal expansion coefficient below and above the T_g becomes less and less evident as the titania content increases, the T_g can be readily determined from the $\ln(Hv) - T$ plots for all hybrid materials (Table 2). A continuous increase of T_g with the filler content can be noted. This result suggests that the micro-Brownian motion of the acrylic network is restricted by the hybridization with the titania network. However, the positive shift of T_g is rather limited (<20 K) and tends to a constant value with the highest titania content.

Actually, the number of groups that can form coordinative bonds with the titania network should be predetermined by the molar content of MA units (i.e. 4 mol%). In this work, all hybrid films have been prepared with a molar excess of Ti with respect to COOH groups of the polymer (see Table 1: Ti/COOH ≥ 2). Therefore, if a quantitative reaction between carboxylic groups of the polymer and titanium butoxide is considered, all the materials prepared in this work should have the same T_g value (same cross-linking density) irrespective of titania content. Actually, the problem here is more complicated, due to the competitive reaction of AcA with the AP in the reaction with the alkoxide. This might explain our peculiar solvent extraction results.

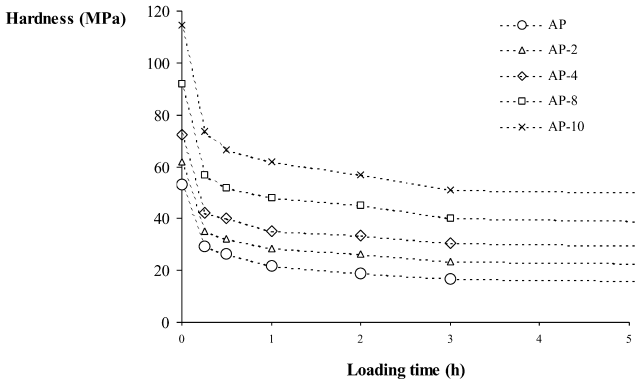

Fig. 8. MH as a function of loading time for hybrid materials with various filler volume fraction (dotted lines are only a guide for the eye).

THF extraction results showed that the percentage of cross-linked polymer increased 2-fold when TiO_2 content increased 6-fold and remained unchanged only for titania content higher than ca. 30% [19]. Although the exact mechanism remains unknown, the latter trend likely results from the increase in the COOTi cross-linked bonds with an increase in the $Ti(OBu)_4$/COOH (from the polymer) molar ratio excess. Above 30% TiO_2, higher $Ti(OBu)_4$/COOH excess do not give more polymer–Ti cross-links. The above discussion reveals a fairly good correlation between the percentage of cross-linked polymer (determined from extraction results) and the T_g of AP in hybrids.

DSC experiments were also carried out to compare the T_g determined from hardness measurements with the T_g determined from the more conventional DSC technique. With all hybrids, the T_g profile in DSC broadens and becomes hardly perceptible. Then, a precise determination of T_g of hybrids from DSC cannot be reasonably expected.

From the T_g of the pure polymer AP determined from DSC technique (Table 2), a positive deviation (ca. 7–11 K) of the experimental value from additivity laws (either the simple rule of mixture or the Fox equation) must be noted. This indicates the presence of specific interactions (hydrogen bondings), which result in a partial loss of chain

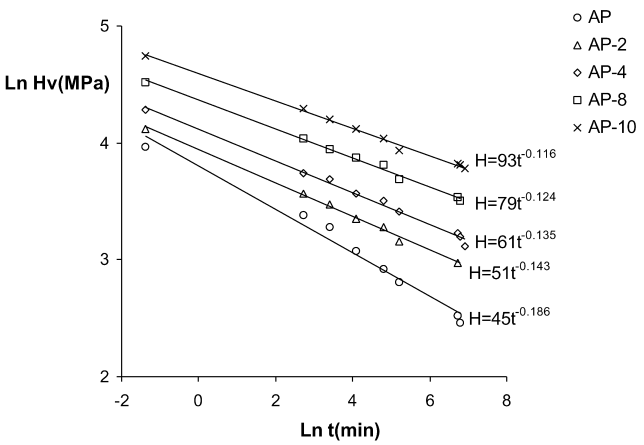

Fig. 9. Double logarithmic plot of MH as a function of loading time for hybrid materials with various filler volume fraction.

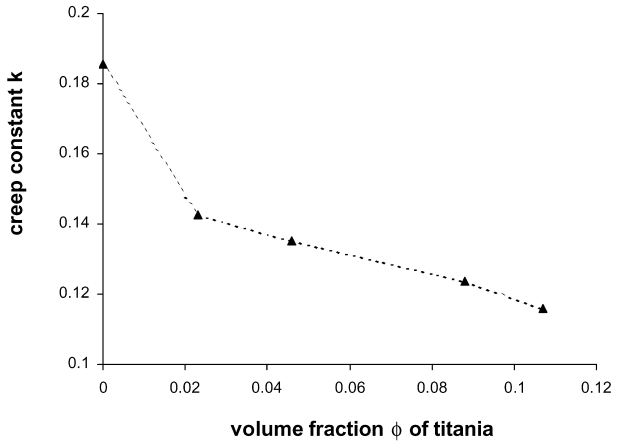

Fig. 10. Variation of creep rate with the volume fraction of titania in hybrid materials (dotted line is only a guide for the eye).

mobility. These hydrogen bondings in the neat polymer might also contribute to the limitation of the positive shift of T_g in the hybrids. Besides, the small difference in the T_g value obtained by MH and DSC (~9 °C) was also reported for poly(methylmethacrylate) and PET polymers [17]: it results from the quasi-static measurement of MH compared to the 10 K/min heating rate used in the DSC scan.

3.6. Creep behavior

To further characterize the effect of the titania content on mechanical properties of composites, the indentation creep behavior of hybrid materials has been studied at room temperature (23 °C).

Fig. 8 shows the variations of hardness with loading time of the investigated hybrids. The continuous decrease (increase) of hardness (diagonal length) clearly reveals the viscoelastic nature of hybrids. The hardness of the investigated materials decreased by as much as 62–78% (depending on the filler content) over a period of 1 day. Over the same period, the associated strain due to creep increases between ca. 62 and 110% depending on the filler content. Fig. 9 shows a double logarithmic plot of MH as a function of loading time. For all hybrid materials, a typical power law function with time is obtained:

$$\mathrm{Hv} = \mathrm{Hv}_0 t^{-k}$$

where Hv_0 is the hardness at $t = 1$ min and k is the so-called creep constant. Such a time-dependent hardness during loading has been previously reported for semi-crystalline [13,36] polymers. In Fig. 10, the value of k is reported as a function of the filler volume fraction. The rate of creep of the material significantly decreases with an increase in filler content. Interestingly, the effect of the filler is more pronounced for the lower filler contents (<2.3 vol%). Compared with the creep rate of the pure AP, the creep rate of the 2.3 vol% filled hybrid decreases by as much as 23%. For higher filler contents, k seems to decrease almost linearly with the volume fraction of titania. $CaCO_3$ in

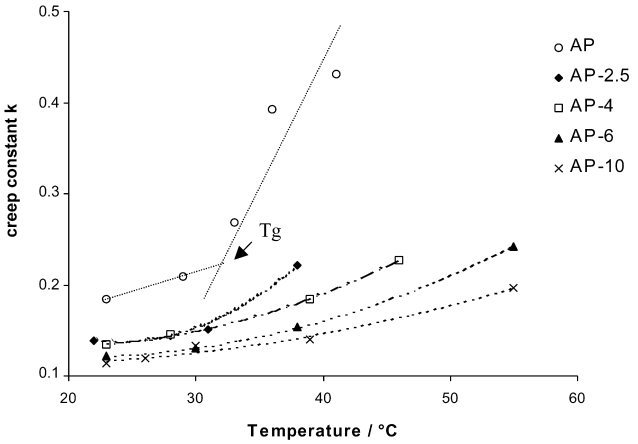

Fig. 11. Variation of creep rate with the temperature for the investigated hybrid materials.

PE–$CaCO_3$ composites was found to have no effect on the creep rate of the polymer at filler volume fraction ranging between 0 and 40% (i.e. log Hv versus log t give straight lines with the same slope for all the investigated materials) [36]. In these composites, the addition of filler only helps in resisting the initial deformation but has no effect afterwards. According to the author [36], the time-dependent process will only be changed if the matrix characteristic is modified. Thus, the change in creep rate observed with acrylic–titania hybrids can be viewed as another evidence of the strong interactions (COOTi coordinative bonds) between the filler and the polymer matrix.

Creep measurements carried out at different temperatures allow to develop another method in determining the T_g of the material. Indeed, with the AP, when temperature increases and reaches a value near T_g, creep rate conspicuously increases (Fig. 11). A T_g of the AP near 305 K can be extrapolated from the $k = f(T)$ data. The latter value fits well with data derived from the low loading time hardness–temperature dependence.

The same trend (increase of k with temperature) is observed with all hybrid materials. However, the bend observed when T reaches T_g becomes less and less evident as the filler content increases. Thus, T_g of the hybrids was not determined due to important potential errors. Fig. 11 also shows that the titania sol–gel network more strongly affect the creep behavior of the polymer above T_g than below T_g. The latter results fit well with previously reported dynamic mechanical properties [19]. Indeed, dynamic mechanical analysis (DMA) revealed a continuous and strong increase of the storage modulus in the rubbery region with the filler content.

This new method for determining T_g suffers from two major drawbacks: firstly, it is time consuming since each value of k was the result of at least eight hardness measurements at loading time varying from 0 to ca. 3 h. Secondly, due to the fast creep at $T \geq T_g$, the indentation size increases too abruptly with time to give reliable hardness values on a sufficiently large time range. Therefore, it is often tricky to determine k above or near T_g.

4. Conclusion

(1) Within the volume fraction range 0–10.7 vol% of titania, a linear relationship between hardness and the volume fraction of titania has been found. Based on the measured hardness of the pure sol–gel titania, the linear relation is suggested to be valid only below the three-dimensional percolation threshold.
(2) The T_g evolution with the titania content follows the same trend as the percentage of cross-linked polymer determined from THF solvent extraction. It was thus suggested that the restriction of polymer chain mobility is mostly due to the strong COOTi bonds in hybrids.
(3) The rate of creep of the hybrids significantly decreases with an increase in titania content, this trend being more significant at a temperature above the T_g of the polymer. This effect is another evidence of the strong interactions between the filler and the AP.
(4) Creep measurements by MH carried out at different temperatures are proposed as a new method to determine the T_g of polymer materials. It gives fair value with the AP but appears too time consuming to be practically effective as a routine method.

Acknowledgements

Grateful acknowledgement is due to Egide for its financial support.

References

[1] Brinker CJ, Sherer GW. Sol–gel science. San Diego: Academic Press; 1990.
[2] Mark JE, Lee CY-C, Bianconi PA, editors. Hybrid organic–inorganic composites. San Diego: ACS Symposium Series; 1995.
[3] Wen J, Wilkes GL. Chem Mater 1996;8:1667.
[4] Landry CJT, Coltrain BK, Landry MR, Fitzgerald JJ, Long VK. Macromolecules 1993;26:3702.
[5] Fitzgerald JJ, Landry CJT, Pochan JM. Macromolecules 1992;25:3715.
[6] Joshua Du Y, Damron M, Tang G, Zheng H, Chu C-J, Osborne JH. Prog Org Coat 2001;41:226.
[7] Wold CR, Soucek MD. Macromol Chem Phys 2000;201:382.
[8] Messaddeq SH, Pulcinelli SH, Santilli CV, Guastaldi AC, Messadeq Y. J Non-Cryst Solids 1999;247:164.
[9] Negele O, Funke W. Prog Org Coat 1996;28:285.
[10] Sugama T, Kukacka LE, Carciello N. Prog Org Coat 1990;18:173.
[11] Balta Calleja FJ. Adv Polym Sci 1985;66:117.
[12] Kajaks J, Flores A, Garcia Guttierez MC, Rueda DR, Balta Calleja FJ. Polymer 2000;41:7769.
[13] Balta Calleja FJ, Santa Cruz C, Asano T. J Polym Sci, Polym Phys 1993;31:557.

[14] Connor MT, Garcia Guttierez MC, Rueda DR, Balta Calleja FJ. J Mater Sci 1997;32:5615.
[15] Balta Calleja FJ, Martinez Salazar J, Asano T. J Mater Sci Lett 1988; 7:165.
[16] Balta Calleja FJ, Santa Cruz C, Sawatari C, Asano T. Macromolecules 1990;23:5352.
[17] Ania F, Martinez-Salzar J, Balta Calleja FJ. J Mater Sci 1989;24:2934.
[18] Fakirov S, Balta Calleja FJ, Krumova M. J Polym Sci, Part B 1999;37: 1413.
[19] Perrin FX, Nguyen V, Vernet JL. Polym Int 2002; in press.
[20] Lebouvier D. L'essai de dureté sur les materiaux revêtus—approche théorique en plasticité et étude expérimentale. PhD Thesis, Paris, 1987.
[21] Low IM, Paglia G, Shi C. J Appl Polym Sci 1998;70:2349.
[22] Bückle ICH. Metall Rev 1959;4:49.
[23] Bückle H. Science of hardness testing and its research applications. Ohio: Westbrook JH and Conrad Metals Park; 1971.
[24] Pethica JB, Tabor D. Surface Sci 1979;89:255.
[25] Mott BW. Micro-indentation testing. London: Butterworths Scientific; 1956.
[26] El-Raghy T, Zavaliangos A, Barsoum M, Kalidindi SR. J Am Ceram Soc 1997;80:513.
[27] Rice RW. J Mater Sci 1979;14:2768.
[28] Suwanprateeb J. Composites; Part A 2000;31:353.
[29] Krumova M, Klingshirn C, Haupert F, Friedrich K. Compos Sci Technol 2001;61:557.
[30] Handbook of chemistry and physics. 55th ed. Cleveland, OH: CRC Press, 1975.
[31] Tabor D. Rev Phys Technol 1970;1:145.
[32] Perrin FX, Nguyen V, Vernet JL. Submitted for publication.
[33] Kuentz M, Leuenberger H. Powder Technol 2000;111:145.
[34] Balta Calleja FJ. Trends Polym Sci 1994;2:419.
[35] Brandrup J, Immergut EH, editors. Polymer handbook, 2nd ed. New York: Wiley; 1975.
[36] Suwanprateeb J. J Mater Sci 1998;33:4917.